Journal of Materials Chemistry A

Accepted Manuscript

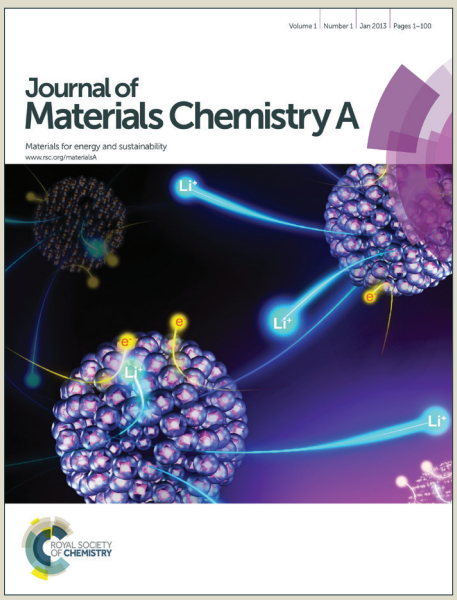

ROYAL SOCIETY OF CHEMISTRY

www.rsc.org/materialsA

Journal Name

RSCPublishing

COMMUNICATION

Fullerene-free organic solar cells with an efficiency of 3.7% based on a low-cost geometrically planar perylene diimide monomer

Cite this: DOI: 10.1039/x0xx00000x

Received 00th January 2012,
Accepted 00th January 2012

DOI: 10.1039/x0xx00000x

www.rsc.org/

R. Singh[a], E.Aulicio-Sarduy[a], Z. Kan[a], T. Ye[a], R.C. I. MacKenzie[b], P. E. Keivanidis[a] *

Abstract

The aggregate-induced limitation for high power-conversion efficiencies (*PCE*s) of perylene-diimide (PDI):polymer solar cells can be circumvented when two simple rules are respected; the aggregate size of PDI remains short enough and the omnipresent PDI aggregates are well electronically-interconnected. Following these guidelines, a *PCE* of 3.7% is delivered by using the solution-processable, planar PDI monomer of N,N'-bis(1-ethylpropyl)-perylene-3,4,9,10-tetracarboxylic diimide as the electron acceptor mixed with the low-energy gap polymeric donor poly[(4,8-bis(5-(2-ethylhexyl)thiophen-2-yl)-benzo[1,2-b;4,5-b']dithiophene)-2,6-diyl-alt-(4-(2-ethylhexanoyl)-thieno[3,4-b]thiophene))-2,6-diyl] (PBDTTT-CT). The PBDTTT-CT:PDI composite absorbs strongly the light in the region of 400 nm – 800 nm and after adding a small amount of 1,8-diiodooctane (DIO) an efficient photocurrent generation is achieved. Space-charge limited dark current and transient photovoltage measurements suggest that the use of the DIO component optimizes the electron/hole carrier mobility ratio, it suppresses the non-geminate recombination losses and it improves the charge extraction efficiency.

Organic solar cells offer the promise of a low cost, low carbon source of energy. Within the last ten years, cell efficiencies have risen from 2% in 2004 [1] to over 11% [2] today. To date, high efficiency solar cells have used fullerene derivatives as the electron acceptor. [3] Although, fullerene derivates have high mobilities and a deep lying LUMO level [4], making them good electron conductors and efficient at separating excitons, their absorption spectrum is poorly matched to that of the solar spectrum preventing them from taking part in light-harvesting. [5] Furthermore, they have low photo-chemical stability, are one of the most expensive components of organic solar cells, and diffuse easily thus offer poor morphological stability. [6] For these reasons, there has been renewed interest in non-fullerene based electron acceptors. [7-11] The identification of alternative efficient n-type molecular architectures is expected to result in improvements not only in organic solar cells, but also other classes of organic electronic devices such as, transistors, photodetectors and bio-sensors where the use of fullerene is a also limiting factor. [12]

Perylene-diimide (PDI) derivatives were among the first n-type materials used in organic solar cells [13, 14] but since the 80's the *PCE* of PDI-based devices have remained inferior to that of fullerene-based devices. [15,16] PDI-derivatives are extremely photostable, absorb efficiently in the visible spectrum, exhibit high electron mobility and crucially their retail cost is much lower than that of fullerenes. [17, 18] However, PDI derivatives tend to aggregate forming long-range ordered PDI aggregates in columnar superstructures. [19] In these structures, excitons convert to intermolecular states that exhibit excimer-like PDI luminescence [20-22] and the well-ordered PDI domains act as charge traps [23] that limit cell efficiency. In our recent work [19] we have suggested that if the PDI columnar aggregates remain short and partially disordered, the dissociation of the slowly diffusive PDI excimers at the PDI/donor interfaces can be efficient and the intercolumnar electron transport is favoured; consequently *PCE*s of close to 2% can be obtained. Recently it was shown that the detrimental effects of PDI columnar stacking in OPV photoactive layers could be minimized if non-planar PDI derivatives such as dimers [24-26] or star-shaped structures [27] are used, and solar cells based on non-planar PDI derivatives have demonstrated *PCE*s of 3% - 4.34%. On the other hand, non-planar PDI derivatives have the disadvantage of requiring many reaction steps that make their synthesis an expensive and a complicated task to achieve; for this reason, utilizing the much lower-cost monomeric PDI derivatives [16, 21] as electron acceptor components in the fabrication protocols of efficient organic solar cells remains an undisputed top-priority that has not yet been accomplished.

In this work we demonstrate that the use of the complex-to-make and costly non-planar PDI-structures is not a necessary requirement for the realization of high *PCE*s in solution-processed organic solar cells. We present evidence that *PCE* values higher than 3.5% are achievable for OPV devices with photoactive layers comprising of the inexpensive, commercially available, planar monomeric form of a PDI derivative mixed with a polymer donor. We mix N,N'-bis(1-ethylpropyl)-perylene-3,4,9,10-tetracarboxylic diimide (PDI) with the low energy gap polymer of poly[(4,8-bis(5-(2-ethylhexyl)thiophen-2-yl)-benzo[1,2-b;4,5-b']dithiophene)-2,6-diyl-alt-(4-(2-ethylhexanoyl)-thieno[3,4-b]thiophene))-2,6-diyl] (PBDTTT-CT). We demonstrate that the PBDTTT-CT:PDI system can deliver a *PCE* of 3.7%. By comparing the electrical properties of the PBDTTT-CT:PDI to reference cells made from the same PDI derivative but mixed with [4,8-bis-substituted-benzo[1,2-b:4,5-b']dithiophene-2,6-diyl-alt-4-substituted-thieno[3,4-b]thiophene-2,6-diyl] (PBDTTT-EO) [19], we are able to identify the origin of the high performance.

The chemical structure of the PBDTTT-CT and PDI materials is presented in Figure 1a.

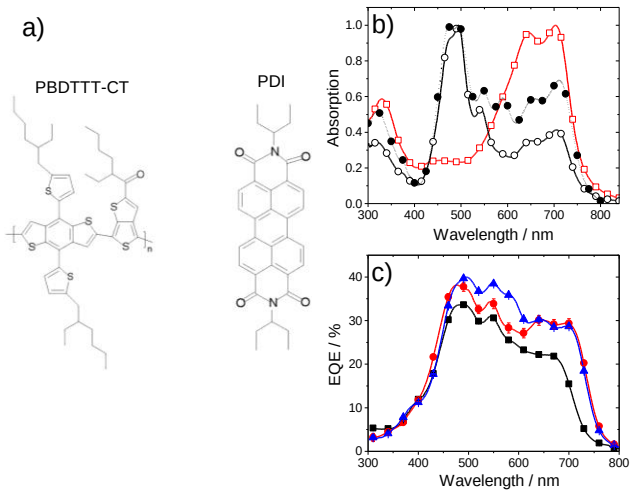

Figure 1. a) The chemical structure of the materials used in this study, b) UV-Vis absorption spectra of a PBDTTT-CT film (open squares), a PBDTTT-CT:PDI 70 wt% film (open circles) and a PBDTTT-CT:PDI 70 wt% w/ 0.4 vol% DIO (filled circles), c) external quantum efficiency spectra devices with photoactive layers of PBDTTT-EO:PDI 70 wt% (squares), PBDTTT-CT:PDI 70 wt% (circles) and PBDTTT-CT:PDI 70 wt% w/ 0.4 vol% DIO (triangles).

Figure 1b presents the UV-Vis spectra of the PBDTTT-CT polymer alone and of the PBDTTT-CT:PDI blend film. In respect to the previously reported UV-Vis spectrum of the PBDTTT-EO:PDI system [19], the PBDTTT-CT:PDI combination covers efficiently the visible spectral range. The absorption spectrum of the PBDTTT-CT polymer donor shifts further to the red by 25 nm and the PBDTTT-CT:PDI blend film has a wider absorption response at lower photon energies. By using a small amount of the 1,8-diiodooctane (DIO) additive the absorption strength of the PBDTTT-CT:PDI blend is increased significantly between 520 nm – 745 nm. The use of additive results in an enhancement of the optical absorption coefficient in the film made by PBCDTTT-CT:PDI with (w/) 0.4 vol% DIO; a 70% increase is found around 745 nm whereas the increase is of 80% around 590 nm.

Figure 1c presents the external quantum efficiency (EQE) spectra of inverted OPV devices with annealed photoactive layers of PBDTTT-EO:PDI, PBDTTT-CT:PDI and PBDTTT-CT:PDI w/ 0.4 vol% DIO. In all cases the geometry of the devices was glass/ITO/ZnO/photoactive layer/V_2O_5/Ag [28] and the devices were annealed at 100 °C for 15 min, after Ag deposition. In respect to the reference device of the PBDTTT-EO:PDI composite, the PBDTTT-CT:PDI system exhibits much higher photocurrent generation efficiency in the spectral region of 475 nm – 750 nm. Moreover, the addition of the DIO additive results in additional enhancement of the EQE of the PBDTTT-CT:PDI device in the spectra region of 520 nm – 640 nm.

The photovoltaic performance of the PBDTTT-CT:PDI system was investigated by the illumination of PBDTTT-CT:PDI devices under simulated solar light (AM1.5G, 98 mW/cm^2). Figure 2a presents the photocurrent density-voltage (*J-V*) characteristics of the PBDTTT-CT:PDI devices with and without DIO. For comparison, the *J-V* curve of the reference PBDTTT-EO:PDI device measured under identical conditions is also shown.

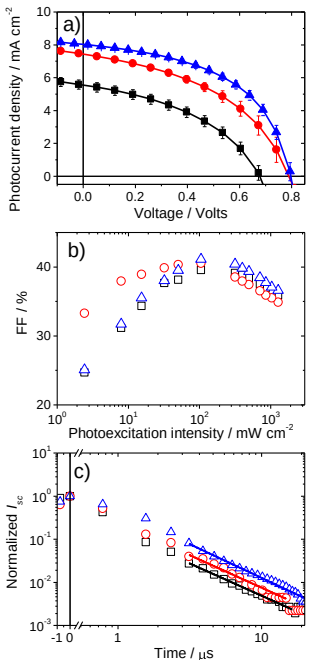

Figure 2. a) *J-V* metrics for devices with a photoactive layer of PBDTTT-EO:PDI 70 wt% (squares), PBDTTT-CT:PDI 70 wt% (circles) and PBDTTT-CT:PDI 70 wt% w/ 0.4 vol% DIO (triangles), b) photoexcitation intensity dependence of the *FF* parameter for devices with photoactive layers of PBDTTT-EO:PDI 70 wt% (squares), PBDTTT-CT:PDI 70 wt% (circles) and PBDTTT-CT:PDI 70 wt% + 0.4 vol% DIO (triangles) after continuous photoexcitation at 532 nm. c) short-circuit current transients for devices with a photoactive layer of PBDTTT-EO:PDI 70 wt% (squares), PBDTTT-CT:PDI 70 wt% (circles) and PBDTTT-CT:PDI 70 wt% w/ 0.4 vol% DIO (triangles). The solid lines are fit to the experimental data (see text).

Table 1 summarizes the main device metrics for these devices, namely the short-circuit current (J_{sc}), the open-circuit voltage (V_{oc}), fill factor (*FF*) and *PCE*.

System	<V_{oc}> (Volts)	<J_{sc}> (mA cm^{-2})	<*FF*> (%)	<*PCE*> (%)	*PCE* $_{max}$ (%)
PBDTTT-EO:PDI	0.70 ± 0.02	5.73 ± 0.09	44.5 ± 0.6	1.79 ± 0.11	1.94
PBDTTT-CT:PDI	0.79 ± 0.01	7.40 ± 0.17	45.0 ± 0.9	2.67 ± 0.12	2.84
PBDTTT-CT:PDI w/ DIO	0.80 ± 0.01	8.10 ± 0.06	51.9 ± 0.7	3.64 ± 0.10	3.71

Table 1. The main device metrics for the devices with photoactive layers of PBDTTT-EO:PDI 70 wt%, PBDTTT-CT:PDI 70 wt% and PBDTTT-CT:PDI 70 wt% w/ 0.4 vol% DIO. For all systems studied 4-6 devices were characterized for confirming the reproducibility of the results obtained.

It can be seen from the device using PBDTTT-CT:PDI has a *PCE* around 1.4 times more than that using PBDTTT-EO:PDI, when the DIO additive is added to the PBDTTT-CT:PDI device, *PCE* increases to around 2.0 times that of the PBDTTT-EO:PDI device. The PBDTTT-CT:PDI w/ 0.4 vol% DIO devices exhibit a *PCE* of 3.7%, and a higher device performance is anticipated after the fine tuning of the layer morphology and the optimization of the device geometry with the use of suitable interlayers. Advantageously, the herein utilized PDI derivative can be obtained on the basis of a far less complex synthetic protocol and it can be already found easily at a low-cost in the market. In addition, the *PCE* of 3.7% is achieved by using only a very small amount of DIO (less than 0.5% vol) which is very promising for enabling an additional reduction in the fabrication cost of efficient PDI-based based OPV devices.

Photoluminescence (PL) quenching characterization of the PBDTTT-CT:PDI films found that in respect to a reference film of poly(styrene) (PS):PDI, the PDI luminescence is quenched by more than 90%. In polymer blend systems of the same monomeric PDI it was found [29] that the overall device efficiency is constrained by a limited dissociation efficiency of the PDI excitons. However, in our systems the majority of PDI monomers are in the form of PDI columnar stacks [19] and most of the PDI excitons are converted instantly to PDI intermolecular states [30] that generate the PDI excimer luminescence. [20-22] Inefficient dissociation of the PDI intermolecular states is expected when the PDI columnar aggregate is larger than the diffusion length of the PDI intermolecular state. [19] In order to verify the effect of the PDI aggregate size on the PL quenching efficiency of the PDI luminescence and to correlate it with the photocurrent generation efficiency of the PBDTTT-CT:PDI devices, we have performed a time-integrated PL spectroscopy study on a set of PBDTTT-CT:PDI composites with increasing content of the DIO additive. In parallel, the surface topography of these samples was studied by atomic force microscopy (AFM) and the photovoltaic properties of the PBDTTT-CT:PDI cells were studied under simulated solar light illumination conditions (AM1.5G, 98 mW/cm^2). In agreement with recent studies on a model polymer:PDI system [31], our results confirm the presence of an anti-correlation between the size of the PDI aggregate and the quenching of the PDI excimer luminescence. In fact, we found that upon increasing the DIO content up to 0.4 vol%, the size of the PDI aggregates is reduced whereas the PL quenching emission of the PDI excimer luminescence and the photocurrent generation efficiency of the corresponding device are increased. For DIO contents higher than 0.4 vol%, the size of the PDI aggregates was found again increased while the PDI PL quenching and the photocurrent generation efficiencies were reduced. (see Supporting Information). As an example, Figure 3 presents the AFM images recorded for the samples of PBDTTT-CT:PDI and PBDTTT-CT:PDI w/ 0.4 vol% DIO.

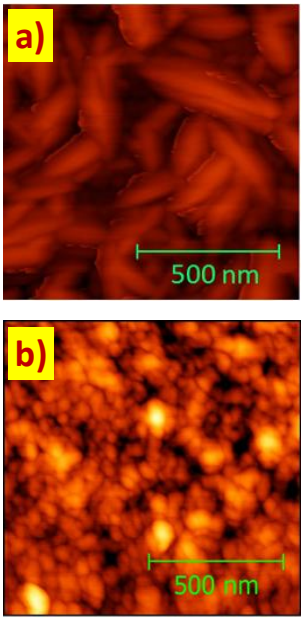

Figure 3. High resolution atomic force microscopy height images for semi complete OPV devices of a) PBDTTT-CT:PDI 70 wt% and b) PBDTTT-CT:PDI 70 wt% w/ 0.4 vol% DIO. In both cases the photoactive layers were deposited onto glass/ITO/ZnO substrates.

The use of the small amount of the DIO additive not only optimizes the size of the PDI aggregates but it also improves the electronic coupling of adjacent PDI aggregates and it helps in balancing the charge transport. We performed space-charge limited current measurements in unipolar devices (see Supporting Information) for determining the electron (μe) and hole (μh) mobility in the three systems. For the PBDTTT-EO:PDI system it was found $\mu_e = 2.9 \times 10^{-6} \pm 1.0 \times 10^{-7}$ cm^2/Vsec and $\mu_h = 4.7 \times 10^{-5} \pm 4.4 \times 10^{-6}$ cm^2/Vsec, in a good agreement with the previously reported values for this system. [19] For the PBDTTT-CT:PDI combination, electron-mobility was found $\mu_e = 6.4 \times 10^{-6} \pm 7.8 \times 10^{-7}$ cm^2/Vsec and hole-mobility was $\mu_h = 8.3 \times 10^{-5} \pm 1.4 \times 10^{-5}$ cm^2/Vsec. The use of the DIO additive for the PBDTTT-CT:PDI systems results in $\mu_e = 7.6 \times 10^{-6} \pm 1.5 \times 10^{-6}$ cm^2/Vsec and $\mu_h = 5.4 \times 10^{-6} \pm 1.9 \times 10^{-6}$ cm^2/Vsec. The observed reduction of the hole mobility after the use of the DIO additive corroborates with the changes observed in the absorption coefficient of the PBDTTT-CT:PDIw/ 0.4 vol% DIO blend film (Figure 1b) that further reflect structural changes in the organization of the polymer chains in the presence of DIO. Its seems that the negative effect of reducing hole mobility, is counterbalanced by the increased light absorption strength at low photon energies and by the optimization of the electron/hole mobility ratio.

Apart from the improvement in the J_{sc} parameter, the *FF* parameter of the PBDTTT-CT:PDI w/ 0.4 vol% DIO surpasses the value of 50% indicating that a device made from this material has both efficient photon harvesting and efficient charge extraction. Figure 2b

presents the intensity dependent *FF* of the three studied OPV systems under monochromatic photoexcitation. Under photoexcitation of 105 mW/cm^2 at 532 nm, the *FF* values increase from PBDTTT-EO:PDI to PBDTTT-CT:PDI and then to PBDTTT-CT:PDI w/ 0.4 vol% DIO, exhibiting $FF_{PBDTTT\text{-}EO:PDI}$= 39.6 %, $FF_{PBDTTT\text{-}CT:PDI}$= 40.5 %, $FF_{PBDTTT\text{-}CT:PDI\ w/\ DIO}$= 41.1 %, in good agreement with the *FF* values obtained after illumination under simulated solar light (Table 1). At higher photoexcitation intensity the *FF* of all three systems decreases indicating the onset of charge recombination. Photoexcitation intensity dependence measurements of the J_{sc} of the PBDTTT-CT:PDI and PBDTTT-CT:PDI w/ 0.4 vol% DIO systems under monochromatic photoexcitation at 532 nm exhibited a linear dependence on photoexcitation intensity verifying that geminate charge recombination is not the main loss channel of device photocurrent for these systems. [25]

Figure 2c presents the photocurrent transients of the PBDTTT-EO:PDI, PBDTTT-CT:PDI and PBDTTT-CT:PDI w/ 0.4 vol% DIO devices generated using a 10 ns long 532 nm optical pulse. In accordance with the time-integrated J_{sc} results (Table 1) the amount of the extracted charge increases upon going from PBDTTT-EO:PDI to PBDTTT-CT:PDI and then to PBDTTT-CT:PDI w/ 0.4 vol% DIO. Interestingly, we found that all three PDI-based OPV cells exhibit photocurrent transients that are best described by a power law function of $I_{sc}(t) \propto I_{sc}(0)^{-\beta}$, where $I_{sc}(t)$ corresponds to the transient photocurrent and $I_{sc}(0)$ corresponds to the photocurrent at t=0. The determined values of the β parameter are $\beta_{PBDTTT\text{-}EO:PDI}$=-1.49, $\beta_{PBDTTT\text{-}CT:PDI}$=-1.51, $\beta_{PBDTTT\text{-}CT:PDI\ w/\ DIO}$=-1.56 for the devices of PBDTTT-EO:PDI, PBDTTT-CT:PDI, PBDTTT-CT:PDI w/ 0.4 vol% DIO, respectively. The prolonged transient photocurrent response in the nanosecond - one microscecond time-scale is attributed to carrier transport whereas at latter times the current is attributed to carriers leaving trap states. [32] The comparable values found for the β parameters suggest that in all three systems the energetic distribution of trap states is the same. [32]

In order to gain further information on the magnitude of non-geminate recombination losses [33], we perform transient photovoltage (TPV) measurements under gradually increased background illumination. During continuous illumination under white light, the cells were photoexcited with 10 ns long pulses of 532 nm light, the results are shown in Figure 4.

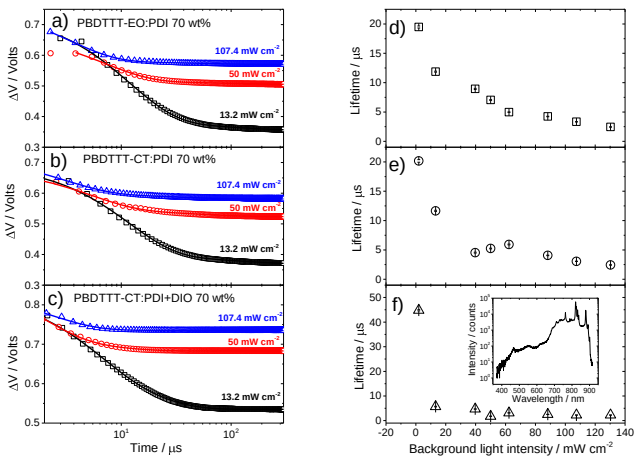

Figure 4. Open-circuit-voltage (V_{oc}) transients for devices with photoactive layers of a) PBDTTT-EO:PDI 70 wt% , b) PBDTTT-CT:PDI 70 wt% and c) PBDTTT-CT:PDI 70 wt% w/ 0.4 vol% DIO (triangles) for background white light illumination intensity of 13.2 mW/cm^2 (squares), 50 mW/cm^2 (circles) and 107.4 mW/cm^2 (triangles). Background white illumination intensity dependent V_{oc} lifetimes of devices with photoactive layers of d) PBDTTT-EO:PDI 70 wt% (squares), e) PBDTTT-CT:PDI 70 wt% (circles) and f) PBDTTT-CT:PDI 70 wt% w/ 0.4 vol% DIO (triangles) The solid lines in a), b) and c) are bi-exponential fits to the experimental data. The inset in f) present the spectrum of the white light used for these measurements.

We found that a bi-exponential was needed to fit the data, possibly due to the different free-electron-to-trapped-hole and free-hole-to-trapped-electron recombination rates. In all cases the dominant carrier lifetime gradually reduces as the background illumination intensity increases. It can be clearly seen that for the case of the PBDTTT-CT:PDI 70 wt% w/ 0.4 vol% DIO device, the lifetime suddenly drops when the light intensity is increased above 10 mW/cm^2, suggesting that the use of DIO additive helps in suppressing bimolecular recombination and increasing charge extraction efficiency, [34] presumably as a result of a faster filling of trap states upon illumination. [35] Close to 1 Sun intensity of background illumination, the carrier lifetime values τ of the three systems are comparable; $\tau_{PBDTTT\text{-}EO:PDI}$= 3.3 μs, $\tau_{PBDTTT\text{-}CT:PDI}$= 3.06 μs, $\tau_{PBDTTT\text{-}CT:PDI\ w/\ DIO}$= 2.3 μs. Further studies are sought for correlating the transient V_{oc} response of the PBDTTT-CT:PDI OPV devices with the microstructure of the photoactive layer [19] and for elucidating the physical meaning of these charge-traps. We note that OPV devices with photoactive layers of the PBDTTT-CT polymer mixed with the phenyl-C_{71}-butyric-acid-methyl ester deliver a *PCE* of 7.6% and a J_{sc}=17.50 mA/cm^2. [36] This suggests that the inferred charge traps in the PBDTTT-CT:PDI system are related mainly with the structural motif of the PDI component and that higher photocurrent generation efficiencies can be reached after gaining a deeper insight on the origin of these charge carrier trapping sites.

Conclusions

In conclusion we have presented evidence that high performance OPV devices can be fabricated by solution-processed polymer blends of commercially available monomeric perylene diimide derivatives when mixed with π-conjugated polymer donors. The use of PDI monomers simplifies greatly the synthetic protocol of these electron-acceptor materials and it maintains the production cost of their photovoltaic devices low. In our study, the device performance of the PBDTTT-CT:PDI OPV system improves greatly after using a small amount of the DIO additive. Transient optoelectronic characterization measurements of the PBDTTT-CT:PDI devices suggest that the efficiency of the organic solar cells prepared by PDI monomeric derivatives is limited by the presence of charge carrier traps. The observed improvement in the device performance, after using the DIO component, is attributed to the increased light absorption of the PBDTTT-CT:PDI composite, to the efficient quenching of the PDI excimer luminescence, to the balanced charge carrier transport and to the elimination of the charge trapping sites in the microstructure of the PBDTTT-CT:PDI photoactive layer. Higher efficiencies for the PDI-based OPV systems can be achieved if the nature and the origin of the inferred charge carrier traps are fully clarified. This could be achieved by correlating trap density and trap depth with the specific microstructure of the OPV layer. Our results offer a paradigm shift in fullerene-free, power-generating polymeric devices and pave the way for inexpensive solution-processed organic solar cells and OPV modules. Tailoring the chemical structure of the PDI core is expected to lead to the next generation of PDI-based optoelectronic devices.

Acknowledgements

The research of PEK that lead to these results has received funding from the People Programme (Marie Curie Actions) of the European Union's Seventh Framework Programme (FP7/2007-2013) under REA grant agreement no PIEF-GA-2011 299657 DELUMOPV. PEK and RM acknowledge the financial support of The Royal Society International Exchanges Scheme - 2013/R3 grant (project 'Understanding how to improve non-fullerene based organic solar cells').

Notes and references

[a] Fondazione Istituto Italiano di Tecnologia, Centre for Nanoscience and Technology@PoliMi, Via Giovanni Pascoli 70/3, 20133 Milano, Italy
[b] University of Nottingham, Department of Mechanical Engineering, UK

† Electronic Supplementary Information (ESI) available: Materials and methods, DIO additive-composition dependent photoluminescence spectra, DIO additive-composition dependent external quantum efficiency spectra, DIO additive-composition dependent device photovoltaic metrics collected under simulated solar illumination (AM1.5G, 0.98 Suns), DIO additive-composition dependent dark *J-V* characteristics and space charge limited current fits. See DOI: 10.1039/c000000x/

1 T. Jeranko, H. Tributsch, N. S. Sariciftci, J. C. Hummelen, Sol. Energ. Mater. Sol. Cells 2004, **83**, 247.
2 M. A. Green, K. Emery, Y. Hishikawa, W. Wartaand, E. D. Dunlop, Prog. Photovolt: Res. Appl. 2014, **22**, 1.
3 R. F. Service, Science 2011, **332**, 293.
4 M. C. Scharber, D. Mühlbacher, M. Koppe, P. Denk, C. Waldauf, A. J. Heeger, C. J. Brabec, Adv. Mater. 2006, **18**, 789.
5 G. F. Burkhard, E. T. Hoke, M. D. McGehee, Adv. Mater. 2010, **22**, 3293.
6 R. Guoqiang, A. Eilaf, S. A. Jenekhe, Adv. Ener. Mater. 2011, **1**, 946.
7 T. Earmme, Y. J. Hwang, N. M. Murari, S. Subramaniyan, S. A. Jenekhe, JACS 2013, 135, 14960.
8 K. Cnops, B. P. Rand, D. Cheyns, B. Verreet, M. A. Empl, P. Heremans, Nat. Comm. 2014, 5, 3406
9 D. Mori, H. Benten, I. Okada, H. Ohkita, S. Ito, Adv. Ener. Mater. 2014, **4**, 1301006
10 J. T. Bloking, T. Giovenzana, A. T. Higgs, A. J. Ponec, E. T. Hoke, K. Vandewal, S. Ko, Z. Bao, A. Sellinger, M. D. McGehee, Adv. Ener. Mater. 2014, doi: 10.1002/aenm.201301426
11 N. Zhou, H. Lin, S. J. Lou, X. Yu, P. Guo, P. Hartnett, H. Huang, M. R. Wasielewski, L. X. Chen, R. P. H. Chang, A. Facchetti, and T. J. Marks Adv. Energy Mater. 2014, doi: 10.1002/aenm.201300785
12 V. Gautam, M. Bag, K. S. Narayan, JACS 2011, **133**, 17942; H. Xu, J. Li, B. H. K. Leung, C. C. Y. Poon, B. S. Ong, Y. Zhang, N. Zhao, Nanoscale 2013, **5**, 11850; K. S. Nalwa, Y. Cai, A. L. Thoeming, J. Shinar, R. Shinar, S. Chaudhary, Adv. Mater. 2010, **22**, 4157
13 P. Panayotatos, D. Parikhi, R. Sauers, G. Bird, A. Piechowski, S. Husain, Solar Cells 1986, **18**, 71.
14 C. W. Tang, Appl. Phys. Lett. 1986, **48**, 183.
15 Schmidt-Mende L., Fechtenkoetter A.,Müllen K., Moons E., Friend R. H., MacKenzie J. D., Science 2001, 293.
16 A. Sharenko, C. M. Proctor, T. S. van der Poll, Z. B. Henson, T.-Q. Nguyen, G. C. Bazan, Adv. Mater. 2013, **25**, 4403
17 Struijk C. W., Sieval A. B., Dakhorst J. E. J., van Dijk M., Kimkes P., Koehorst R. B. M., Donker H., Schaafsma T. J., Picken S. J., van de Craars A. M., Warman J. M., Zuilhof H., Sudhoelter E. J. R., J. Am. Chem. Soc. 2000, **122**, 11057.
18 X. Zhan, A. Facchetti, S. Barlow, T. J. Marks, M. A. Ratner, M. R. Wasielewski, S. R. Marder, Adv. Mater. 2011, **23**, 268
19 T. Ye, R. Singh, H.-J. Butt, G. Floudas, P. E. Keivanidis, ACS Appl. Mater. Interfaces 2013, **5**, 11844.
20 Z. Chen, U. Baumeister, C. Tschierske, F. Wurthner, Chem. Eur. J. 2007, **13**, 450.
21 P. E. Keivanidis, I. A. Howard, R. H. Friend, Adv. Funct. Mater. 2008, **18**, 3189.
22 I. A. Howard, F. Laquai, P. E. Keivanidis, R. H. Friend, N. C. Greenham, J. Phys. Chem. C 2009, **113**, 21225.
23 S. Foster, C. E. Finlayson, P. E. Keivanidis, Y. S. Huang, I. Hwang, R. H. Friend, M. B. J. Otten, L. P. Lu, E. Schwartz, R. J. M. Nolte, A. E. Rowan, Macromolecules 2009, **42**, 2023.
24 S. Rajaram, R. Shivanna, S. K. Kandappa, K. S. Narayan, The Journal of Physical Chemistry Letters 2012, **3**, 2405.
25 R. Shivanna, S. Shoaee, S. Dimitrov, S. K. Kandappa, S. Rajaram, J. Durrant, K. S. Narayan, Energy Environ. Sci. 2013, **7**, 435
26 X. Zhang, Z. Lu, L. Ye, C. Zhan, J. Hou, S. Zhang, B. Jiang, Y. Zhao, J. Huang, S. Zhang, Y. Liu, Q. Shi, Y. Liu, J. Yao, Adv. Mater. 2013, 25, 5791; Z. Lu, B. Jiang, X. Zhang, A. Tang, L. Chen, C. Zhan, J. Yao, Chem. Mater. 2014, DOI: 10.1021/cm5006339
27 Y. Lin, Y. Wang, J. Wang, J. Hou, Y. Li, D. Zhu, X. Zhan, Adv. Mater. 2014, DOI: 10.1002/adma.201400525
28 I. Hancox, L. A. Rochford, D. Clare, P. Sullivan, T. S. Jones, Appl. Phys. Lett. 2011, **99**, 013304
29 D. Gehrig, I. A. Howard, V. Kamm, C. Dyer-Smith, F. Etzold, F. Laquai, in Proc. SPIE 8811, Physical Chemistry of Interfaces and Nanomaterials XII, 88111F, 2013.
30 A. Schubert, V. Settels, W. Liu, F. Würthner, C. Meier, R. F. Fink, S. Schindlbeck, S. Lochbrunner, B. Engels, V. Engel, J. Phys. Lett. 2013, **4**, 792
31 Singh R., Giussani E., Mróz M. M., Di Fonzo F., Fazzi D., Cabanillas-González J., Oldridge L., Vaenas N., Kontos A. G., Falaras P., Grimsdale A. C., Jacob J., Müllen K., Keivanidis P. E., Organic Electronics, 2014, **15**, 1347.
32 R. C. I. MacKenzie, C. G. Shuttle, G. F. Dibb, N. Treat, E. von Hauff, M. J. Robb, C. J. Hawker, M. L. Chabinyc, J. Nelson, J. Phys. Chem. C 2013, **117**, 12407.
33 C. G. Shuttle, B. O'Regan, A. M. Ballantyne, J. Nelson, D. D. C. Bradley, J. de Mello, J. R. Durrant, Appl. Phys. Lett. 2008, **92**, 093311

34 C. M. Proctor, S. Albrecht, M. Kuik, D. Neher, T.-C. Nguyen, Adv. Ener. Mater. 2014, doi: 10.1002/aenm.201400230
35 R. C. I. MacKenzie, T. Kirchartz, G. F. A. Dibb, J. Nelson, J. Phys. Chem. C 2011, **115**, 9806
36 L. Huo, S. Zhang, X. Guo, F. Xu, Y. Li, J. Hou, Angew. Chem. Int. Ed. 2011, **50**, 9697